CrossMark

ORIGINAL PAPER

# Evolution of atmospheric boundary layer structure and its relationship with air quality in Wuhan, China

Yassin Mbululo [1,2] · Jun Qin [1] · Zheng Xuan Yuan [1]

**Abstract** Air pollution data, air quality index (AQI) data and L-band sounding data of Wuhan City from January 1 to February 28, 2015, were used in this study. Since air quality is mainly determined by the condition of the atmospheric boundary layer structure (ABLS), a detailed analysis was carried out in order to determine the evolution of this layer and its relationship with air quality. During the investigation period, the highest value of AQI was 307 on January 26 and the lowest was 33 on February 28 indicating 'severe pollution' and 'excellent' air quality, respectively. The concentrations of $PM_{2.5}$ during the days with the highest and lowest AQI were 142.61 and 9.78 $\mu g/m^3$, respectively. The percentage of days in which the ratio of $PM_{2.5}$ in $PM_{10}$ was more than half was 83.05% which means that the greater portion of pollutants were composed of smaller particles. Moreover, four $PM_{2.5}$ episodes (three or more consecutive days of $PM_{2.5} \geq 75$ $\mu g/m^3$) were identified and the average percentage of elementary carbon (EC) in $PM_{2.5}$ during episode 1 (prior to the episode) was 6.274% (6.276%), episode 2 was 5.634% (7.174%), and episode 4 was 4.067% (7.785%). Higher concentrations of EC prior to episodes suggest biomass burning to be one of the reasons for episodes occurrence. Analysis of the ABLS during polluted days show that the boundary layer was dry and warm and had weak low-level wind and dominance of northerly winds. A different scenario is seen on clean days as the boundary layer is observed to be wet and cool, and there is dominance of strong winds. Back trajectory analysis results show that polluted days were dominated by air mass from north China while on clean days, the dominant air masses were from East China Sea, Mongolia, and west China.

**Keywords** Air pollution · Air quality · Atmospheric boundary layer structure · Episode

## Introduction

A recent report by the World Health Organization (WHO) revealed that only one person in every ten lives in a city complying with the WHO air quality guidelines. Moreover, newly released estimates show that outdoor air pollution alone kills about 3 million people each year, mainly from non-communicable diseases, while the blend of outdoor and indoor air pollution is responsible for about one in every nine deaths annually (WHO 2016). China, as the fastest-growing country with a lot of industries, is facing a serious problem of air pollution in most of its cities. So far, it is the world's largest emitter of black carbon (Streets et al. 2001; Wang et al. 2012). As it has been revealed by Li and Zhang (2014), this has been attributed mostly to the use of coal as one of the power sources for industries and the heating source in most households. To mitigate this, the strict National Ambient Air Quality Standard (NAAQS) was enacted by the Chinese Ministry of Environmental Protection (MEP) in 2012 to regulate the emission of air pollutants such as $NO_2$, $SO_2$, CO, $O_3$ and particulate matter (PM) to the atmosphere. $PM_{10}$ is the particulate matter with an aerodynamic diameter of less than 10 $\mu m$, and $PM_{2.5}$ is the particulate matter with an aerodynamic diameter of less than 2.5 $\mu m$. The upper limits for annual average $PM_{10}$ and $PM_{2.5}$ are 70 and 35 $\mu g/m^3$, respectively, while their

✉ Jun Qin
   qinjunnj@126.com

   Yassin Mbululo
   ymbululo@suanet.ac.tz

[1] Institute of Atmospheric Physics and Atmospheric Environment, School of Environmental Studies, China University of Geosciences, Wuhan, China

[2] Solomon Mahlangu College of Science and Education, Sokoine University of Agriculture, Morogoro, Tanzania

24-h averages are 150 and 75 μg/m$^3$, respectively (GB3095-2012 2012). It is worth noting that this is the first time PM$_{2.5}$ is included in the NAAQS (Zhang and Cao 2015; Fu et al. 2016) which is universally used as proxy indicator of exposure to air pollution (WHO 2016). Wuhan City and other cities in China adopted this stringent law and started using the new air quality index (AQI) for ranking air pollution since 2013.

According to the China national population census of 2010, Wuhan City (114° E, 30° N) had a population of 8.36 million people (Zeng et al. 2015). The city lies in central China and is referred to as the 'heart' of the country due to its uniqueness in geographical location (Weiwei et al. 2006). Moreover, major transport routes (railways and roads) connecting eastern and western China together with the Yangtze river pass through the city. With its popular slogan of 'Wuhan, different every day', the city is not only different every day in terms of economic developments, but also in terms of the increase in air pollution level. Around the city, construction works are almost everywhere, and a good number of traffic and manufacturing activities have resulted in an increasing number of air pollution sources. A number of studies have reported the air of Wuhan to be polluted (Weiwei et al. 2006; Zhangxiong et al. 2014; Lyu et al. 2015; Lyu et al. 2016; Wang et al. 2016a) mostly during winter (Song et al. 2016). This is attributed to both the increase in coal burning in most households as the source of heat (Zhang et al. 2008; Lyu et al. 2015) and the unfavourable meteorological conditions which limit the dispersion and mixing of air pollutants (Xu et al. 2011; Han et al. 2014; Zhang and Cao 2015). Nevertheless, atmospheric boundary layer (ABL) structure is an important factor which needs to be taken into consideration when analysing surface concentrations of air pollutants (Zhou et al. 2005; Wu et al. 2013; Hu et al. 2014). As defined by Holtslag et al. (1985), ABL is the lower part of the troposphere which is in continuous interaction with the earth's surface due to friction and heating or cooling. It is generally characterized by the turbulence and diurnal cycles of temperature, wind, specific humidity and other tracers particularly on land. Since it has the capability of mixing air with different properties efficiently, then, the representation of the turbulence directly impacts the atmosphere and the air quality (Holtslag 2015). Moreover, the height of ABL over land varies significantly over time; it is higher during the daytime due to surface heating from shortwave radiation and lower during the night-time (Zhou et al. 2005; Wu et al. 2013; Hu 2015). A study by Quan et al. (2013) found higher concentration of aerosol when the BL height is low and lower concentration when it is high. This is because lower BL height depresses the dispersion of aerosol leading to the increase in aerosol concentration.

A number of studies have been conducted recently with regard to the air quality in Wuhan. Song et al. (2016) revealed that before 2013, there was a notable increase of the number of days with good air quality in Wuhan but soon after the implementation of the new NAAQS, in which PM$_{2.5}$ was considered, the number dropped abruptly. Moreover, average monthly variations of SO$_2$, NO$_2$ and PM$_{10}$ during the period between 2001 and 2014 were much higher during winter and lower during other seasons. Another study by Lyu et al. (2016) on chemical characteristics reveal that the quality of air in Wuhan was polluted since PM$_{10}$ and PM$_{2.5}$ frequently exceeded NAAQS due to intensive biomass burning. The authors report the average concentrations of PM$_{2.5}$ to be 81.2 and 85.3 μg/m$^3$ in summer and autumn, respectively. Six air pollution episodes were identified during the investigated period as a result of intensive biomass burning and fugitive dust. Wang et al. (2016a, 2016b) found the annual average concentrations of PM$_{2.5}$, PM$_{10}$ and NO$_2$ exceeding the NAAQS by 256, 192 and 137%, respectively. For the case of monthly average, they found the highest value of PM$_{2.5}$ to be in December as a result of local emission and the lowest in July as a result of precipitation. The average concentrations of PM$_{2.5}$ were 42.1, 124.5 and 268.0 μg/m$^3$ during clean air, haze and heavy-haze periods, respectively. A study on indoor and outdoor pollutants in autumn and winter by Lu et al. (2011) found average outdoor (indoor) concentrations of PM$_{2.5}$ of 137.0 μg/m$^3$ (104.2 μg/m$^3$) in winter and 104.2 μg/m$^3$ (91.3 μg/m$^3$) in autumn. Air pollutants in both scenarios were higher outdoors than indoors and also higher in winter than autumn. These results suggest that the buildings serve as barriers to PM$_{2.5}$ and prevent it from invading the indoor environment. Furthermore, analysis of trace metals in PM$_{10}$ by Weiwei et al. (2006) found high levels of As, Cd, Mn, Pb and Zn compared to other Asian cities and high proportions of Ni and Cr in addition to the aforementioned trace metals compared with EU cities. The major sources of these trace metals were identified to be smelting, coal combustion, traffic and steel manufacture. Nevertheless, the correlation coefficients of daily average organic carbon (OC) and elementary carbon (EC) during a typical haze in Wuhan were found to be 0.83 and 0.99 in May and June, respectively, which indicate their source to be complex in May and single in June (Zhangxiong et al. 2014). The major source of pollution event was identified to be biomass burning.

Based on the literature the authors came across, it is clear that most of the studies which have been done so far in Wuhan have not given enough attention to the atmospheric boundary layer structure (ABLS). Most of the atmospheric pollutants are released in the ABL, and the quality of air depends strongly on the mixing capability of this turbulent buffer which couples the surface with the free troposphere (Tennekes 1974; Quan et al. 2013; Kong and Yi 2015; Petäjä et al. 2016; Wang et al. 2016b). This study, therefore, aims at improving the knowledge base by (a) analysing the air quality and (b) studying the evolution of ABLS during the pollution process in Wuhan based on the ground observation data from a meteorological station, high-altitude sounding data and air quality data.

**Table 1** Grading standards of air quality

| Air quality index (AQI) | Air quality index level | Air quality index category |
|---|---|---|
| 0~50 | Level 1 | Excellent |
| 51~100 | Level 2 | Good |
| 101~150 | Level 3 | Slightly polluted |
| 151~200 | Level 4 | Moderate polluted |
| 201~300 | Level 5 | Heavy pollution |
| > 300 | Level 6 | Severe pollution |

Source: HJ633–2012 (2012)

## Materials and methods

This study used L-band radar sounding data that were provided by Wuhan Meteorological Bureau. The daily observation time for L-band radar was 0700 hours LST at a vertical resolution of 10 m. The vertical profile of different meteorological variables (temperature, relative humidity, wind speed and direction) from the ground up to 3000 m was then used to describe the ABLS. Ground observation data from Wujiashan meteorological station was also made available. This study also used AQI data and air quality data ($PM_{10}$, $PM_{2.5}$, OC, EC, $NO_2$, and $SO_2$) which were provided by Wuhan Environmental Protection Agency (WHEPA). Details on how AQI is calculated have been elaborated clearly on HJ633-2012 (2012). Daily averaged data for AQI and $PM_{2.5}$ from January 1 to February 28, 2015, were then used to plot the line graph from which one could define highly polluted and clean days; L-band sound data were used to plot the vertical profile of the meteorological variables. The evolution of ABLS and the pollutants was further studied during the pollution process.

In addition to this, hybrid single-particle Lagrangian integrated trajectory (HYSPLIT) model developed by National Oceanic and Atmospheric Administration (NOAA) Air Resources Laboratory's (ARL) of the USA was used to calculate and analyse airflow and diffusion trajectories (Stein et al. 2015; Rolph 2017). The model has relatively complete transport, diffusion and sedimentation models for handling a variety of meteorological element input fields, multiple physical processes and different types of pollutant emission sources (http://www.arl. noaa.gov/HYSPLIT.php). In this study, HYSPLIT-WEB was used to track air trajectories of Wuhan for 72 h, with a view to the qualitative description of the air transport path during the pollution process. Meteorological data input was from the National Centers for Environmental Prediction (NCEP) fields obtained from NOAA which is available at every 3 h with 1° × 1° spatial resolution. Three different levels (100, 300 and 600 m) were set at the model to determine the specific transport path of air mass during identified pollution process.

## Results and discussion

### Air quality analysis

The average AQI in January and February was 158 which indicates the condition of the air to be moderately polluted (Table 1), and the primary pollutant was $PM_{2.5}$ in all the days except for January 1 and February 9 when the primary pollutants were $PM_{10}$ and $NO_2$, respectively. The percentage of days in which the ratio of $PM_{2.5}$ to $PM_{10}$ was more than half was found to be 83.05% (49 out of 59 days) which signifies that a greater portion of pollutants were composed by small particles. A previous study by Wang et al. (2016a, 2016b) reported the same scenario as they found for the whole year; $PM_{2.5}$ was contributing 66.4% of $PM_{10}$. An experimental study by Doronzo et al. (2011) shows that fine particles have the tendency of being lofted up by thermal convection while the coarse particles tend to settle down once they lose the momentum. These small particles are thought to have serious negative consequences to human health and the atmosphere because of their large specific surface area (Wang

**Fig. 1** Daily average $PM_{2.5}$ and AQI for January and February 2015. Episodes 1, 2 and 3 are found in January and episode 4 in February. Blue horizontal line shows the limit for 24-h average concentration of $PM_{2.5}$. The combination of episode 1 and 2 is making a pollution process which was further studied
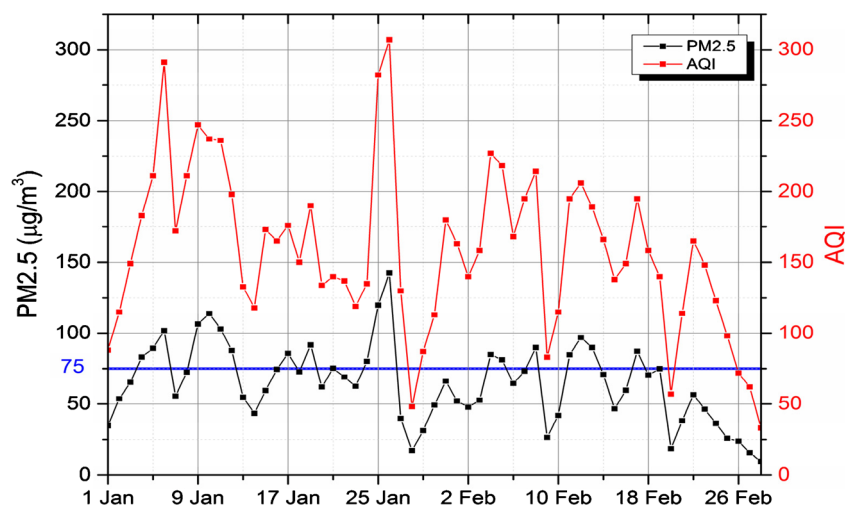
**Table 2** Correlation coefficient ($r$) between OC, EC, and $PM_{2.5}$ daily means

| Item | OC | EC | EC/OC | OC/$PM_{2.5}$ | EC/$PM_{2.5}$ | $PM_{2.5}$ |
|------|----|----|-------|---------------|---------------|------------|
| OC | 1 | 0.62709 | − 0.01351 | − 0.0936 | − 0.06118 | 0.71587 |
| EC |  | 1 | 0.74563 | − 0.41246 | 0.31713 | 0.78528 |
| EC/OC |  |  | 1 | − 0.5405 | 0.45543 | 0.42287 |
| OC/$PM_{2.5}$ |  |  |  | 1 | 0.27865 | − 0.57178 |
| EC/$PM_{2.5}$ |  |  |  |  | 1 | − 0.28381 |
| $PM_{2.5}$ |  |  |  |  |  | 1 |

et al. 2015; Lyu et al. 2016). Furthermore, only 9 days (15.25%) out of 59 days were found to be clean (levels 1 and 2). Based on NAAQS (GB3095-2012 2012), Fig. 1 presents the average daily concentration of $PM_{2.5}$ in Wuhan City where 13 days (41.9%) in January and 7 days (25%) in February are seen to be above the daily acceptable level. The highest (maximum) value of AQI ($PM_{2.5}$) within these 2 months was 307 (142.61 $\mu g/m^3$) on January 26 indicating 'severe pollution', and the lowest (minimum) value of AQI ($PM_{2.5}$) was 33 (9.78 $\mu g/m^3$) on February 28 indicating 'excellent' air quality. Generally, this has been attributed to meteorological conditions at the ABL which were observed during these days and transboundary movement of air pollutants from the heavily polluted area of northern China. During these 2 months, four $PM_{2.5}$ episodes (three or more consecutive days of $PM_{2.5} \geq 75$ $\mu g/m^3$) were identified, three in January and the fourth one in February. Episode 1 occurred between January 4 and 6, episode 2 between January 9 and 11, episode 3 between January 24 and 26 and episode 4 between February 11 and 13.

Moreover, most combustion processes tend to emit fine carbonaceous matter generating two major components: EC and OC. Turpin and Huntzicker (1999) revealed OC to be of greater concern as it is associated with mutagenic and carcinogenic effects and can be emitted directly from the source (primary) or produced from atmospheric reactions (secondary OC). These carbonaceous species are among the major components of $PM_{2.5}$ in Wuhan as it was found that the average concentration of OC within $PM_{2.5}$ is 20.38 $\mu g/m^3$ and the chemical variation within the $PM_{2.5}$ was observed to be higher in the preceding days of episodes than the episode days. The fraction of EC in $PM_{2.5}$ during episode 1 was 6.274% ± 0.515% (mean ± standard deviation), episode 2 was 5.634% ± 0.612% and episode 4 was 4.067% ± 0.813% while 3 days prior to the episodes were 6.276% ± 0.7677, 7.174% ± 1.409 and 7.785% ± 3.934%, respectively. Data of EC on episode 3 was not captured; therefore, its fraction was not calculated. Since EC is the tracer element of incomplete combustion (Wu and JZ 2016), therefore, a higher concentration of EC observed prior to episodes 1, 2 and 4 suggests that biomass burning is the reason for the occurrence of this pollution on these days.

The minimum OC/EC ratio was found to be 3.50 on January 9, and the maximum ratio was 24.237 on February 28. These observed higher ratios are not a surprise because OC accounts for a large portion of aerosols, which are found at

**Table 3**    Ground meteorological element during heavily polluted days (AQI $\geq$ 201)

| Date | Air temperature (°C) | Humidity (%) | Wind speed (m/s) | Wind direction | Pressure (hPa) | Characteristics of the inversion layer | | |
|------|----------------------|--------------|------------------|----------------|----------------|----------------------------------------|---|---|
| | | | | | | Strength (°C/100 m) | Altitude (m) | Thickness (m) |
| 05-01-15 | 12 | 68 | 1 | 203 | 1008 | 2.4 | 0 | 190 |
| 06-01-15 | 7.1 | 80 | 4 | 23 | 1020 | 1.29 | 730 | 140 |
| 08-01-15 | − 0.6 | 97 | 1 | 68 | 1029 | 4 | 0 | 150 |
| 09-01-15 | 1.9 | 98 | 0 | C | 1027 | 5.67 | 0 | 90 |
| 10-01-15 | 3 | 98 | 0 | C | 1026 | 4.08 | 0 | 120 |
| 11-01-15 | 2.6 | 98 | 0 | C | 1025 | 4.14 | 0 | 140 |
| 25-01-15 | 5.1 | 97 | 2 | 338 | 1019 | 2 | 470 | 110 |
| 26-01-15 | 5.6 | 72 | 1 | 360 | 1019 | 0.54 | 490 | 240 |
| 04-02-15 | − 2 | 98 | 1 | 338 | 1030 | 2.81 | 0 | 160 |
| 05-02-15 | − 2.5 | 98 | 1 | 338 | 1031 | 2.17 | 0 | 240 |
| 08-02-15 | 0.4 | 87 | 3 | 23 | 1029 | 2.43 | 0 | 70 |
| 12-02-15 | 3 | 95 | 2 | 158 | 1015 | 3 | 0 | 300 |
| Average | 2.97 | 90.5 | 1.33 | 205.44 | 1023.17 | 2.87 | 563.33[a] | 162.5 |

[a] Average of the suspended inversions

**Table 4**  Ground meteorological element during clean days (AQI ≤ 100)

| Date | Air temperature (°C) | Humidity (%) | Wind speed (m/s) | Wind direction | Pressure (hPa) | Characteristics of the inversion layer | | |
|---|---|---|---|---|---|---|---|---|
| | | | | | | Strength (°C/100 m) | Altitude (m) | Thickness (m) |
| 01-01-15 | − 3.2 | 80 | 2 | 45 | 1032 | 6.5 | 0 | 80 |
| 28-01-15 | − 0.1 | 93 | 3 | 23 | 1025 | 0.33 | 540 | 270 |
| 29-01-15 | − 0.9 | 97 | 2 | 45 | 1026 | Nil | Nil | Nil |
| 09-02-15 | 0.3 | 85 | 1 | 113 | 1030 | 1.47 | 0 | 170 |
| 20-02-15 | 4.9 | 97 | 1 | 360 | 1014 | 0.78 | 370 | 230 |
| 25-02-15 | 9.1 | 98 | 1 | 23 | 1012 | 0.09 | 220 | 110 |
| 26-02-15 | 8.4 | 98 | 2 | 23 | 1016 | 0.55 | 0 | 110 |
| 27-02-15 | 8.3 | 98 | 2 | 23 | 1014 | Nil | Nil | Nil |
| 28-02-15 | 1.3 | 96 | 3 | 23 | 1024 | 0.07 | 1140 | 140 |
| Average | 3.12 | 93.56 | 1.89 | 75.33 | 1021.44 | 1.4 | 567.5[a] | 158.57 |

[a] Average of the suspended inversions

urban centres (Turpin and Huntzicker 1999). A number of studies have regarded the OC/EC ratio of above 2 as a good indicator of the existence of secondary organic aerosol (Chow et al. 1996; Turpin and Huntzicker 1999) even though the source and formation mechanism of this secondary organic aerosol are still debatable among the scientific community (Huang et al. 2010; Wu and JZ 2016). Furthermore, a preceding study by Lyu et al. (2016) in Wuhan during summer also suggests the presence of secondary organic carbon due to high OC/EC ratio. Therefore, these higher ratios signify the presence of secondary organic aerosol in $PM_{2.5}$ on both episode and non-episode days while the higher values during episode days suggested the formation of secondary organic aerosols. Han et al. (2014) suggest the highest ratios which are observed after the episode days to be the results of accumulation of pollutants due to atmospheric stability. The correlation coefficients ($r$) between OC, EC and $PM_{2.5}$ during January and February were found to be 0.71587 and 0.7853, respectively, while the correlation coefficient of OC and EC was found to be 0.62709 (Table 2). As it has been explained by Zhangxiong et al. (2014) and Gu et al. (2010), this observed correlation suggests the complexity of OC and EC sources.

### Analysis of atmospheric boundary layer structure

Evolution analysis of ABLS over Wuhan City during winter was described based on the L-band sounding data of different meteorological variables such as temperature, humidity and wind direction and speed. The structure and variation characteristics of the averaged ABL for polluted and clean days were summarized, and the meteorological reasons for the occurrence of pollution events are analysed in the subsequent subsection.
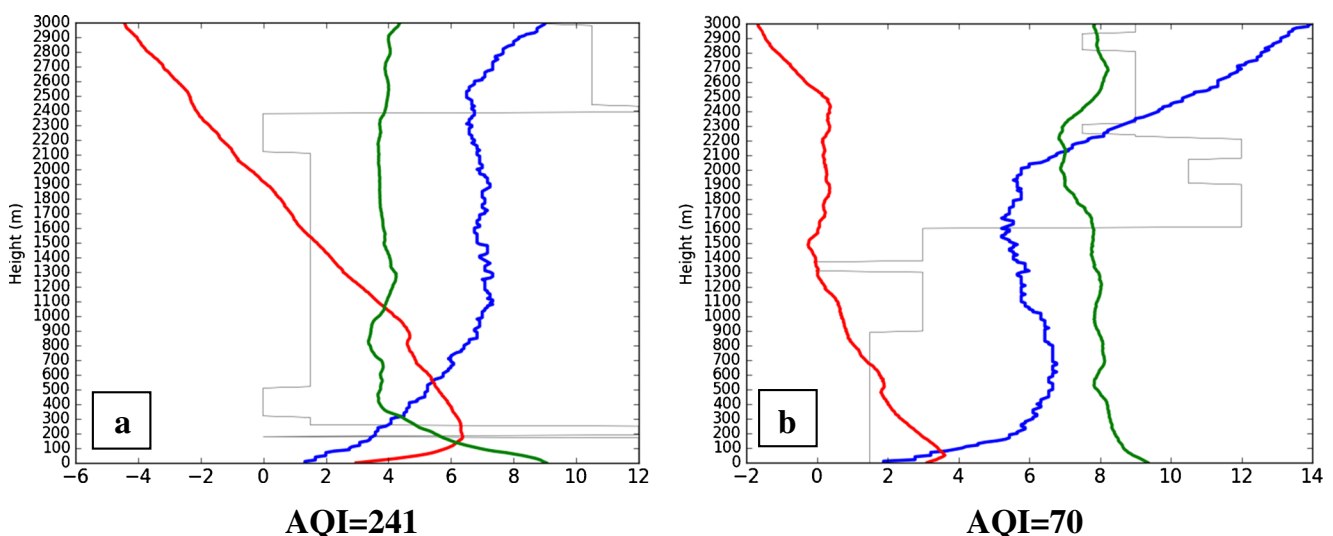


**Fig. 2  a, b** Averaged vertical structure of the atmosphere showing the profile of temperature (red line, °C), relative humidity (green line, %), wind velocity (blue line, m/s), and wind direction (grey line) for polluted and clean days. The number on the x-axis is the result after dividing the relative humidity value by 10 and wind direction angle by 30 while temperature and wind speed remain the same

**Table 5** Average AQI and pollutants during polluted and clean days

|          | AQI | $PM_{2.5}$ | $PM_{10}$ | $O_3$ | $SO_2$ | NO | $NO_2$ | CO | OC | EC |
|----------|-----|------------|-----------|-------|--------|-----|--------|------|-------|------|
| Polluted | 241 | 100.17 | 147.74 | 17.65 | 36.34 | 65.40 | 85.92 | 4.09 | 25.38 | 5.62 |
| Clean | 70 | 22.62 | 34.31 | 29.67 | 11.80 | 10.85 | 32.53 | 1.53 | 11.63 | 1.57 |

*Averaged boundary layer structure for clean and polluted days*

Summary statistics of the ground meteorological variables show that there is no any significant difference between polluted and clean days (Tables 3 and 4). Nevertheless, a clear distinction can be seen on the characteristics of the inversion layer, such as the strength of the inversion layer and the number of occurrence of ground inversion. This is because the quality of air depends mostly on the ABL rather than the ground meteorological conditions (Hu 2015). The averaged boundary layer (BL) for 12 days, which was found to be 'heavily polluted' (AQI ≥ 201) as described in the grading standard of air quality (Table 1), showed a ground temperature of 2.97 °C and a very strong ground inversion with a temperature increase rate of 2.87 °C/100 m (Table 3 and Fig. 2a). Near the ground, relative humidity was 90.5% and at about 400~900 m, it was reduced to about 40%. The wind at the ground was weak, with an average speed of about 1.33 m/s, and it increased at an average angle of 45° up to the altitude of 1100 m where it attained the speed of about 7.0 m/s, which was maintained up to the altitude of about 2600 m. Wind direction near the ground was in the N direction, and above the altitude of 500 m, it maintained the NNE direction up to the altitude of 2100 m. Moreover, Table 5 shows the averaged AQI to be 241 and the primary pollutants to be $PM_{2.5}$ with an average concentration of 100.17 μg/m³ which is far above the daily acceptable limit. Together with this, averaged concentrations of $NO_2$ and CO were also above the daily acceptable limits of 80 and 4.0 mg/m³, respectively.
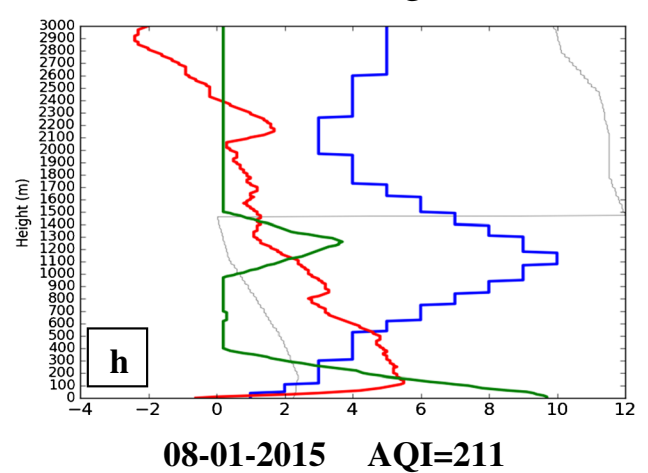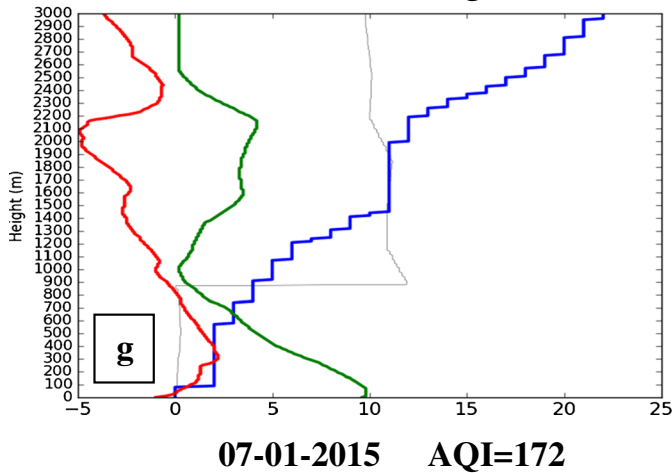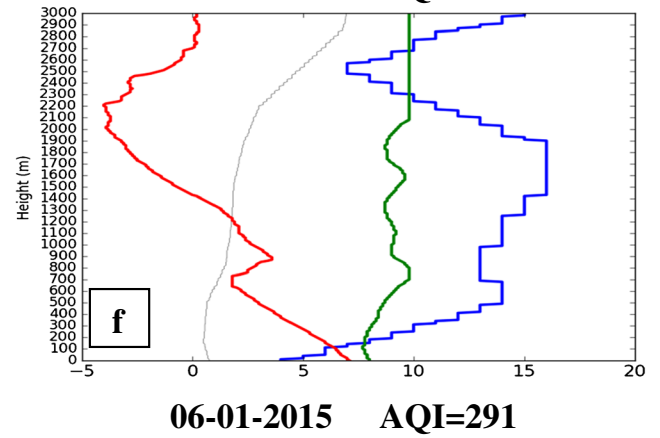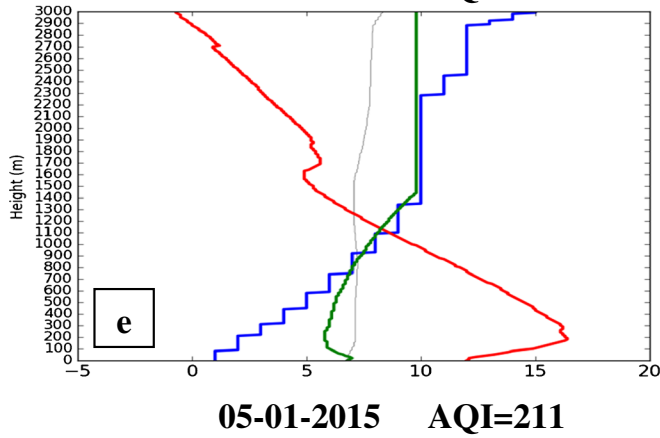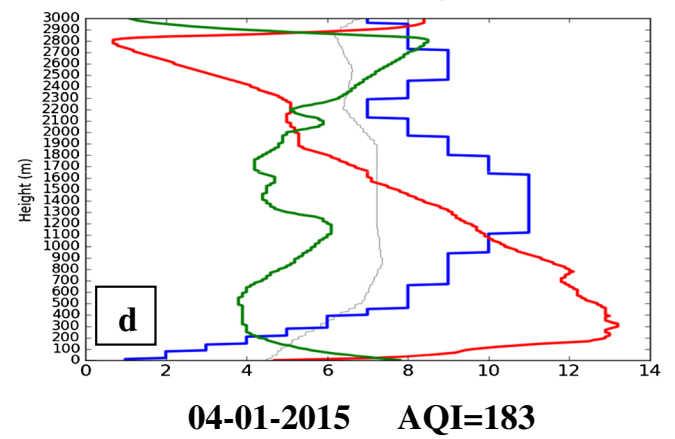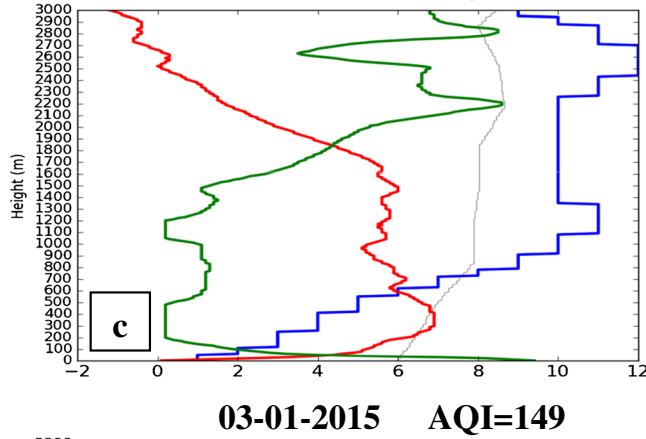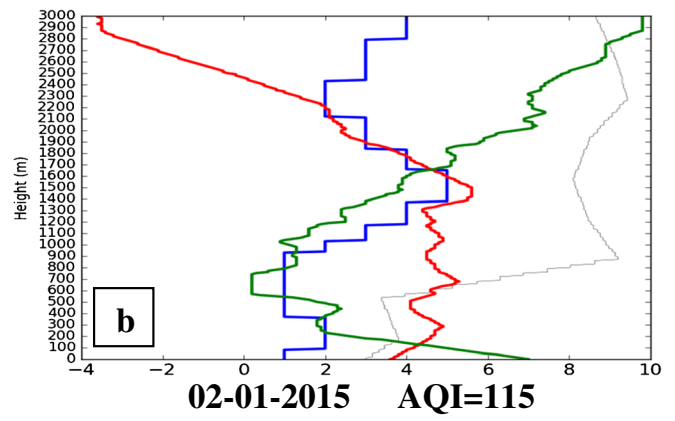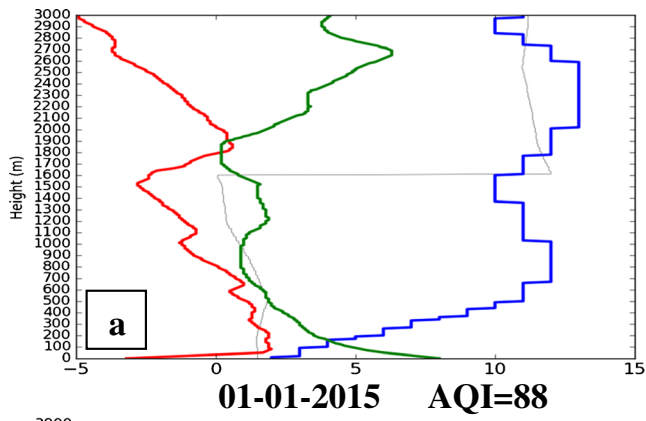
A different scenario can be seen on the averaged clean days as the averaged AQI was 70 indicating a 'good' air quality (Table 1), and the primary pollutant was $PM_{2.5}$ with an averaged concentration of 22.62 μg/m³ which is far below the daily acceptable limit. Six principle pollutants together with the carbonaceous pollutants were also far below the acceptable limit. Furthermore, a very small ground inversion with thickness of about 50 m is seen at the averaged ABLS (Table 4 and Fig. 2b). Above it, there is a constant temperature drop up to the altitude of about 500 m where another inversion layer of thickness of about 50 m is seen to develop and the temperature continues to drop up to the altitude of 1500 m. A wind speed of about 1.89 m/s is observed at the surface, which increased rapidly to about 7 m/s at the altitude of 500 m. The BL is seen to be humid with the average amount of about 80~90% which indicates the cleanliness of the whole layer. The wind direction from the ground surface to 900 m is NNE, and at around 1600~1900 m, it maintained N after a clockwise rotation.

The above analysis shows that in polluted days, the BL is dry and warm, wind speed is low and the wind direction near the ground is N. Meanwhile, during clean days, the BL is wet and cool, wind speed is high and the wind direction near the ground is NNE. Note that the direction of the wind is one of the important factors in determining the air quality in Wuhan because there is a big coal-fired power station in NNE (Yangluo power station) and the polluted areas are always in the downwind side of the pollutant sources. These general characteristics of the ABLS during polluted (clean) days are unfavourable (favourable) for dispersion and mixing of the pollutants because weak winds near the ground result into weak horizontal transport capacity. Additionally, the presence of the strong inversion layer near the ground halts vertical transport capacity; as a result, pollutants are forced to remain suspended near the ground surface.

*Analysis of pollution process on episode 1*

During the investigated period, an observable air pollution process is seen from January 1 to 14, 2015, with a total number of 14 days. Figure 3a–n shows the vertical structure of the ABL during heavy-pollution process with daily meteorological variables at 0700 hours. On January 1 at 0700 hours, the ABLS is seen to be dry, relative humidity on the ground is about 80% and it dropped to about 9% at 740 m (Fig. 3a). A thin and strong inversion layer below 80 m and a series of suspended inversion layers in the whole BL are seen. This was a peculiar day as it was the only day which recorded $PM_{10}$ as the primary pollutant with an average concentration of 68.79 μg/m³. The average concentrations of other pollutants such as $PM_{2.5}$, $NO_2$, $SO_2$ and $O_3$ were 34.68, 48.68, 37.82 and 38.64 μg/m³, respectively. The dominance of larger particles which have high settling velocity due to the influence of gravity and the presence of strong winds reached a maximum speed of about 12 m/s at an altitude of 670~1020 m, resulting in good air quality. Apart from the larger particles, a 72-h air mass back trajectory shows the existence of air mass from northwest China which crosses through Xinjiang and Inner Mongolia (Fig. 4a), the places which are characterized

**Fig. 3** Vertical structure of the atmosphere showing the profile of ▶ temperature (red line, °C), relative humidity (green line, %), wind velocity (blue line, m/s), and wind direction (grey line) during the pollution process. The number on the x-axis is the result after dividing the relative humidity value by 10 and wind direction angle by 30 while temperature and wind speed remain the same
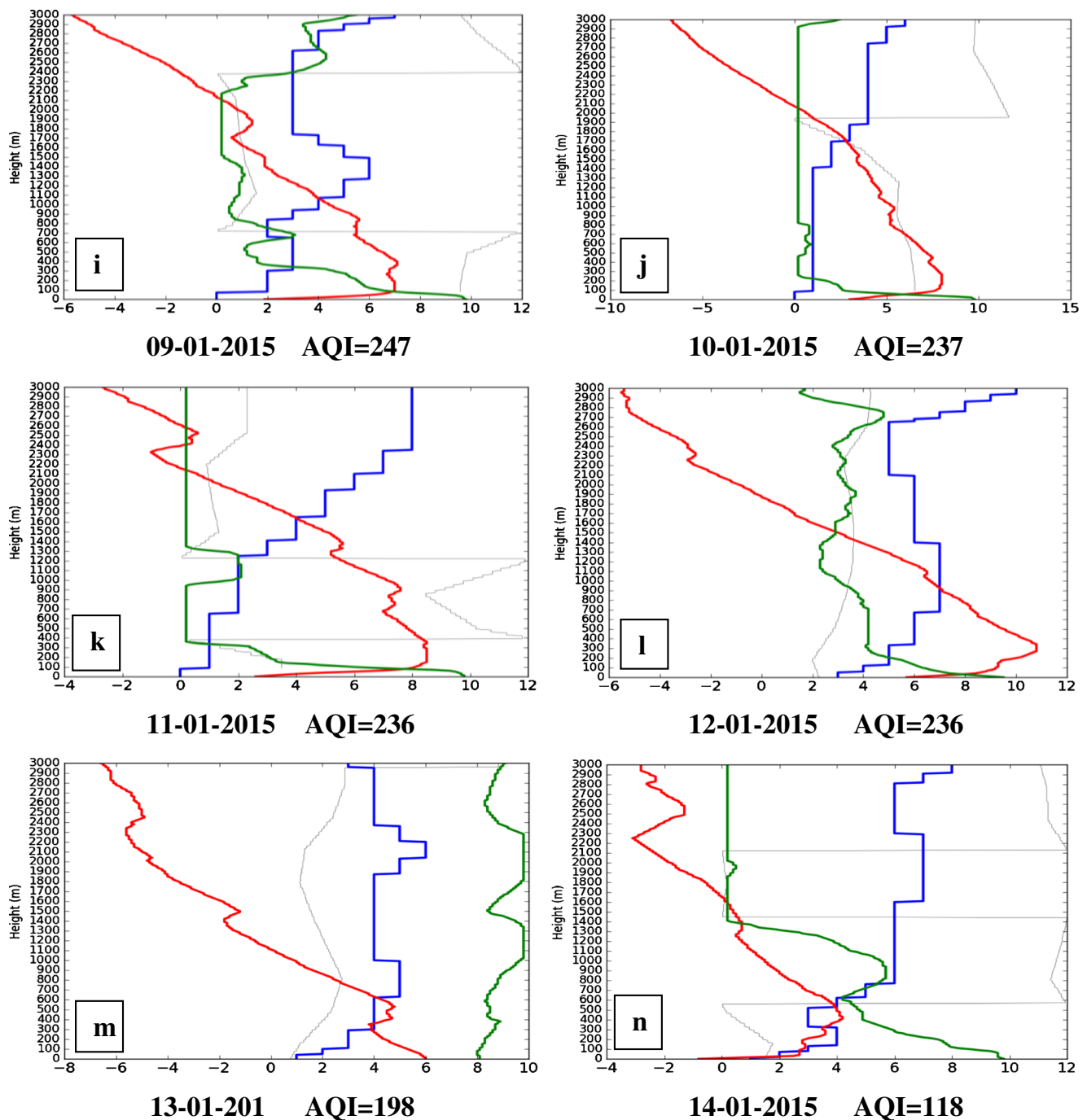
**01-01-2015    AQI=88**

**02-01-2015    AQI=115**

**03-01-2015    AQI=149**

**04-01-2015    AQI=183**

**05-01-2015    AQI=211**

**06-01-2015    AQI=291**

**07-01-2015    AQI=172**

**08-01-2015    AQI=211**

**09-01-2015    AQI=247**



**10-01-2015    AQI=237**



**11-01-2015    AQI=236**



**12-01-2015    AQI=236**



**13-01-201    AQI=198**



**14-01-2015    AQI=118**

**Fig. 3** (continued)

by cold air and strong wind. Strong winds are an important factor as they sustain horizontal transportation of the pollutants which are found within the boundary layer. An AQI of 88 was recorded, and the air quality was categorized as 'Good' (Table 1). The most significant changes began to be seen from January 2 at 0700 hours, when the concentrations of $PM_{2.5}$, $NO_2$, and $SO_2$ increased by 54.75, 44.56 and 32.84%, while concentrations of $PM_{10}$ and $O_3$ decreased by 1.08 and 80.63%, respectively. The primary pollutant on this day was $PM_{2.5}$, which has the characteristic of settling slowly.

Furthermore, ground inversion layer with thickness of 290 m and a series of suspended inversion layers are seen to be developed. The BL was warm, and the wind speed was weak, reaching a maximum speed of 5 m/s at the altitude of 1380 m (Fig. 3b). Horizontal dispersion capacity was seen to be weakened significantly, and the air quality during this day was deteriorated and recorded an AQI of 115, which was categorized as 'slightly polluted'.

The intensity of the inversion layer was seen to strengthen from January 2 to 5 (Fig. 3b–e), while on January 6 a

significant change was observed in the meteorological variables at the BL as compared to the previous days (Fig. 3f). During this day, there was no ground inversion as it was the case for the previous days up to the altitude of 730~890 m, and the whole BL is seen to be wet. The wind direction was mainly northerly, and its speed was seen to increase significantly, reaching a maximum speed of 14 m/s at an altitude of 490 m. The primary pollutant during this day was $PM_{2.5}$ with a concentration of 101.85 μg/m$^3$, while the concentrations of

$NO_2$, $SO_2$ and $O_3$ were 66.11, 31.41 and 9.09 μg/m$^3$, respectively. Compared to the previous days, the condition of the BL looked to be better and it was expected that the air quality will improve, but surprisingly, this day was recorded as the second most polluted day with AQI of 291 and it was categorized as 'heavily polluted'. Results from the 72-h back trajectory (Fig. 4b) show that low-level winds originated from Beijing-Tianjin-Hebei (BTH), the area which has been reported by Cao et al. (2012) and Zhang et al. (2017) as the most polluted
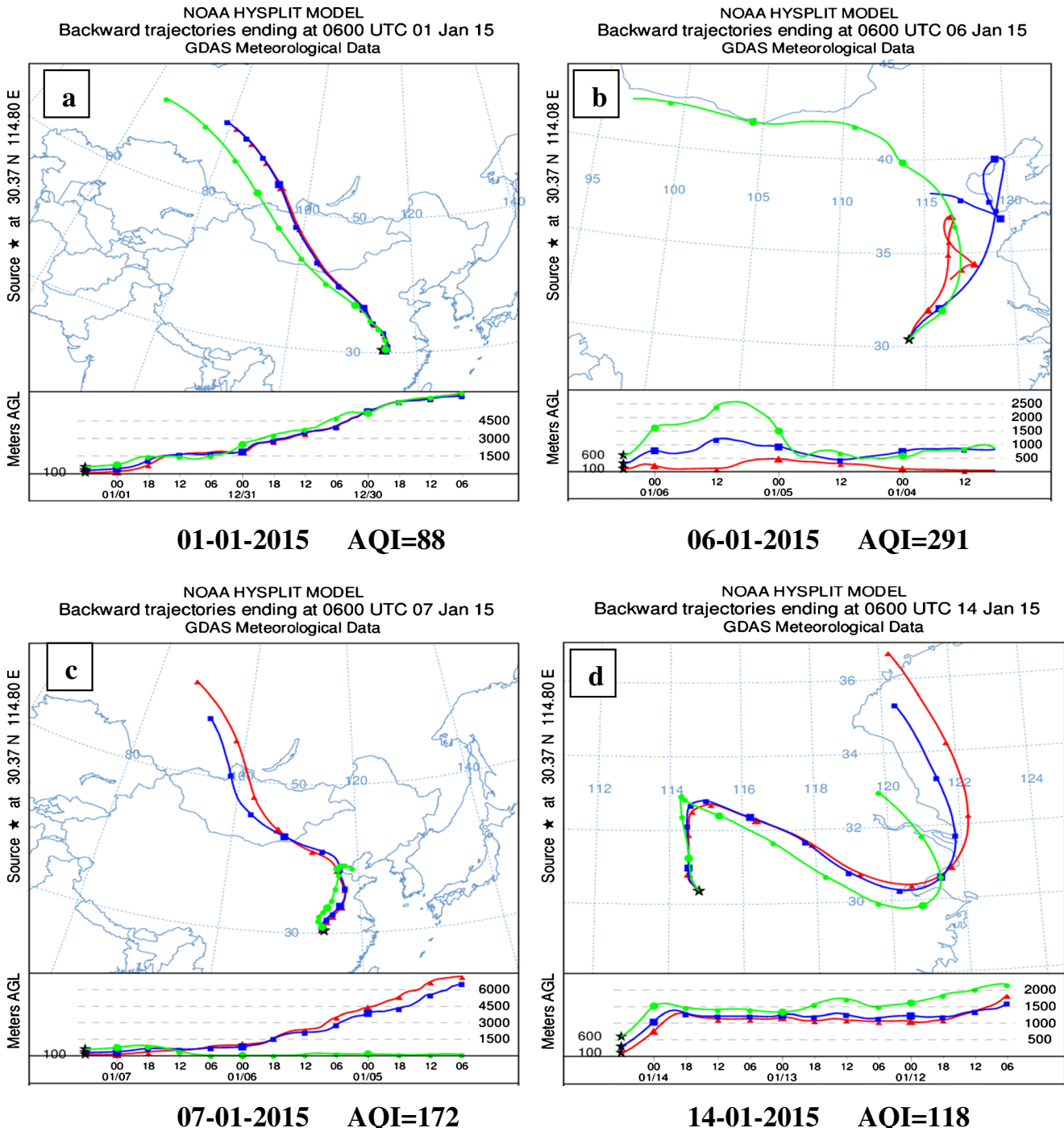


**01-01-2015    AQI=88**

**06-01-2015    AQI=291**

**07-01-2015    AQI=172**

**14-01-2015    AQI=118**

**Fig. 4**  Air mass backward trajectory for 72 h at altitudes of 100, 300 and 600 m of the selected date during pollution process

area in China. This observation shows the transboundary movements of air pollutants affect the air quality regardless of the state of ABL which appears to be favourable for diffusion of pollutants of local origin. Therefore, the source of the air mass plays an important role in determining the air quality of Wuhan. Furthermore, this day was the peak point for this pollution process and the pollutant accumulation was at its maximum level, partially due to the stability and long lifetime of $PM_{2.5}$ (Lyu et al. 2016). On January 7 at 0700 hours, an AQI of 172 (moderate pollution) was recorded which is a significant improvement in air quality as compared to the previous day, even though a ground inversion layer with a thickness of 300 m was observed (Fig. 3g). A 72-h back trajectory shows that the air mass source during the day was from the southern part of Russia and crossed Mongolia before it entered the most polluted area of BTH (Fig. 4c). The decline in pollutants is partially due to the source of these winds being cold and strong and the settling rate. Furthermore, the relative humidity within the first 420 m was about 50~96% and above this altitude, it just declined significantly, reaching 2% at an altitude of 1000 m. The dominant wind direction up to an altitude of 800 m was northerly wind with low speed.

*Analysis of pollution process of episode 2*

Two days before January 9 at 0700 h, which is the starting point of episode 2, an intensification of the inversion layer was observed, which resulted into the worsening of air quality (Fig. 3g–i). On this day, an AQI of 247 which can be categorized as 'heavy pollution' was recorded. From January 10 to 12 at 0700 hours, there was no significant change in AQI and BL meteorological conditions. During these 3 days, the AQI was 236 to 237 which can be categorized as 'heavy pollution' as well. Figure 3j–l shows very strong ground inversions, low relative humidity and low wind speed near the ground. A day later, on January 13 at 0700 hours, an AQI of 198 (moderate pollution) was recorded, when the ground inversion layer disappeared (Fig. 3m) and the whole BL was wet (80~98%).

A different scenario was observed on January 14 at 0700 hours, when a strong ground inversion layer was developed up to the altitude of 410 m and AQI of 118 (Slightly polluted) was recorded (Fig. 3n). The primary pollutant was $PM_{2.5}$ with a concentration of 43.32 $\mu g/m^3$, while the concentrations of $NO_2$, $SO_2$ and $O_3$ were 57.33, 11.68 and 22.69 $\mu g/m^3$, respectively. Relative humidity in the first 600 m was about 40~98%, and the wind speed was low at the BL. A 72-h back trajectory of air mass shows that the low-level air masses are transported from the Yellow Sea and East China Sea via Shanghai and Anhui (Fig. 4d). The origin of these air masses and route is clean, that is why there is significant improvement of air quality during this day.

## Conclusion

Data of air pollution, Air quality index, L-band sounding and back trajectory results were used in this study to investigate the evolution of ABLS of Wuhan City. The average condition of air quality of Wuhan shows that the city is 'moderately polluted' which is equivalent to level 4. The primary pollutant during these 2 months of investigation was $PM_{2.5}$, except on January 1 and February 9 when the primary pollutants were $PM_{10}$ and $NO_2$, respectively. Moreover, four $PM_{2.5}$ episodes were found; three in January (4 to 6, 9 to 12 and 24 to 26) and the fourth one in February (11 to 13). Higher ratios of carbonaceous species were observed prior to the $PM_{2.5}$ episodes than during the episodes, which suggests biomass burning to be one of the reasons why $PM_{2.5}$ episode occurred during those days. Moreover, minimum and maximum ratios of OC/EC were 3.5 and 24.237, respectively, which indicates that a large portion of $PM_{2.5}$ was composed of OC. The first and second $PM_{2.5}$ episodes formed a single pollution process which was further studied by analysing the evolution of the meteorological variables on BL. Summary statistics of ground meteorological variables show that there was no significant difference between polluted and clean days, but rather, a clear distinction can be seen on the characteristics of the inversion layer and the number of occurrence of ground inversion. Furthermore, during polluted days, there was weak horizontal wind below the BL and strong temperature inversion which resulted in limited vertical dispersion of pollutants. The BL was mainly dry and warm, and the direction of wind was mainly northerly. A different scenario was observed at the BL during clean days as it was mainly wet and cool. The wind speed near the ground was much stronger. Likewise, back trajectory results show the dominance of air mass from the most polluted region of BTH during polluted days, while there is dominance of air masses from East China Sea, Mongolia and the western part of the country during clean days. These results imply that the source of air mass plays a significant role in determining the air quality of Wuhan. Nevertheless, improved conditions of the ABLS also favour vertical dispersion and horizontal mixing of air pollutants. It is also worth acknowledging the contribution of emissions from large-scale infrastructure and construction activities as one of the major contributors of air pollution observed, even though their contribution was not quantified in this study.

# References

Cao JJ, Shen ZX, Chow JC, Watson JG, Lee SC, Tie XX, Ho KF, Wang GH, Han YM (2012) Winter and summer PM2.5 chemical compositions in fourteen Chinese cities. J Air Waste Manage Assoc 62: 1214–1226. https://doi.org/10.1080/10962247.2012.701193

Chow JC, Watson JG, Lu Z, Lowenthal DH, Frazier CA, Solomon PA, Thuillier RH, Magliano K (1996) Descriptive analysis of PM2.5 and PM10 at regionally representative locations during SJVAQS/AUSPEX. Atmos Environ 30:2079–2112

Doronzo DM, De TMD, Dellino P, Pascazio G (2011) Numerical simulation of pyroclastic density currents using locally refined Cartesian grids. Comput Fluids 44:56–67. https://doi.org/10.1016/j.compfluid.2010.12.006

Fu X, Cheng Z, Wang S, Hua Y, Xing J and Hao J (2016) Local and regional contributions to fine particle pollution in winter of the Yangtze River Delta, China. 2001:1067–1080. doi: https://doi.org/10.4209/aaqr.2015.08.0496

GB3095-2012 (2012) People's Republic of China National Ambient Air Quality Standard. 1–12

Gu J, Bai Z, Liu A, Wu L, Xie Y, Li W, Dong H (2010) Characterization of atmospheric organic carbon and element carbon of PM2.5 and PM10 at Tianjin, China. Aerosol Air Qual Res 10:167–176. https://doi.org/10.4209/aaqr.2009.12.0080

Han SQ, JH W, Zhang YF, Cai ZY, Feng YC, Yao Q, Li XJ, Liu YW, Zhang M (2014) Characteristics and formation mechanism of a winter haze-fog episode in Tianjin, China. Atmos Environ 98:323–330. https://doi.org/10.1016/j.atmosenv.2014.08.078

HJ633-2012 (2012) People's Republic of China, National Environmental Protection Standard, Technical requirements for ambient air quality index (AQI) (trial implementation) 1–6

Holtslag AAM (2015) Modeling and parameterization. Boundary layer (atmospheric) and air pollution, 2nd editios. Encyclopedia of Atmospheric Sciences, Elsevier, pp 265–273

Holtslag AAM, Gryning SE, Irwin JS and Sivertsen B (1985) Parameterization of the atmospheric boundary layer for air pollution dispersion models. In: Wispelaere C De, Schiermeier FA and Gillani N V (eds) Air pollution modelling and its application V Springer Science, pp 147–174

Hu XM (2015) Air pollution meteorology. Boundary layer (atmospheric) and air pollution, 2nd Edition. Encyclopedia of Atmospheric Sciences, Elsevier, pp 227–236

Hu XM, Ma Z, Lin W, Zhang H, Hu J, Wang Y, Xu X, Fuentes JD, Xue M (2014) Impact of the Loess Plateau on the atmospheric boundary layer structure and air quality in the North China Plain: a case study. Sci Total Environ 499:228–237. https://doi.org/10.1016/j.scitotenv.2014.08.053

Huang X, Zhao Q, He L, Hu M, Bian Q, Xue L, Zhang Y (2010) Identification of secondary organic aerosols based on aerosol mass spectrometry. Sci China Chem 53:2593–2599. https://doi.org/10.1007/s11426-010-4088-7

Kong W, Yi F (2015) Convective boundary layer evolution from lidar backscatter and its relationship with surface aerosol concentration at a location of a central China megacity. J Geophys Res Atmos 120: 7928–7940. https://doi.org/10.1002/2015JD023248

Li M, Zhang L (2014) Haze in China: current and future challenges. Environ Pollut 189:85–86. https://doi.org/10.1016/j.envpol.2014.02.024

Lu M, Fan Y, Yao S, Mingquan H, Masayuki S, kenji t (2011) Indoor and outdoor characteristics of particulate matter and OC, EC in autumn and winter in Wuhan. Urban Environ Urban Ecol 24:25–32

Lyu XP, Wang ZW, Cheng HR, Zhang F, Zhang G, Wang XM, Ling ZH, Wang N (2015) Chemical characteristics of submicron particulates (PM1.0) in Wuhan, Central China. Atmos Res 161:169–178. https://doi.org/10.1016/j.atmosres.2015.04.009

Lyu XP, Chen N, Guo H, Zeng L, Zhang W, Shen F, Quan J, Wang N (2016) Chemical characteristics and causes of airborne particulate pollution in warm seasons in Wuhan, central China. Atmos Chem Phys 16:10671–10687. https://doi.org/10.5194/acp-16-10671-2016

Petäjä T, Järvi L, Kerminen V-M, Ding AJ, Sun JN, Nie W, Kujansuu J, Virkkula A, Yang X, CB F et al (2016) Enhanced air pollution via aerosol-boundary layer feedback in China. Sci Rep 6:18998. https://doi.org/10.1038/srep18998

Quan J, Gao Y, Zhang Q, Tie X, Cao J, Han S, Meng J, Chen P, Zhao D (2013) Evolution of planetary boundary layer under different weather conditions, and its impact on aerosol concentrations. Particuology 11:34–40. https://doi.org/10.1016/j.partic.2012.04.005

Rolph GD (2017) Real-time environmental applications and display system (READY) website (http://www.ready.noaa.gov). NOAA Air Resources Laboratory, College Park, MD

Song J, Guang W, Li L and Xiang R (2016) Assessment of air quality status in Wuhan, China Atmosphere (Basel) doi: https://doi.org/10.3390/atmos7040056

Stein AF, Draxler RR, Rolph GD, Stunder BJB, Cohen MD, Ngan F (2015) NOAA's HYSPLIT atmospheric transport and dispersion modeling system. Bull Am Meteorol Soc 96:2059–2077. https://doi.org/10.1175/BAMS-D-14-00110.1

Streets DG, Gupta S, Waldhoff ST, Wang MQ, Bond TC, Bo YY (2001) Black carbon emissions in China. Atmos Environ 35:4281–4296. https://doi.org/10.1016/S1352-2310(01)00179-0

Tennekes H (1974) The atmospheric boundary layer. Phys Today 27:52–63. https://doi.org/10.1063/1.3128397

Turpin BJ, Huntzicker JJ (1999) Identification of secondary organic aerosol episodes and quantitation of primary and secondary organic aerosol concentrations during SCAQS. Atmos Environ 29:3527–3544

Wang R, Tao S, Wang W, Liu J, Shen H, Shen G, Wang B, Liu X, Li W, Huang Y et al (2012) Black carbon emissions in China from 1949 to 2050. Environ Sci Technol 46:7595–7603. https://doi.org/10.1021/es3003684

Wang J, Wang S, Voorhees AS, Zhao B, Jang C, Jiang J, JS F, Ding D, Zhu Y, Hao J (2015) Assessment of short-term PM2.5-related mortality due to different emission sources in the Yangtze River Delta, China. Atmos Environ 123:440–448. https://doi.org/10.1016/j.atmosenv.2015.05.060

Wang S, Yu S, Yan R, Zhang Q, Li P, Wang L, Liu W, Zheng X (2016a) Characteristics and origins of air pollutants in Wuhan, China, based on observations and hybrid receptor models. J Air Waste Manage Assoc 2247:10962247.2016.1240724. https://doi.org/10.1080/10962247.2016.1240724

Wang W, Mao F, Gong W, Pan Z, Du L (2016b) Evaluating the governing factors of variability in nocturnal boundary layer height based on elastic lidar in Wuhan. Int J Environ Res Public Health 13:1071. https://doi.org/10.3390/ijerph13111071

Weiwei L, Yanxin W, Xavier Q, Xinguo Z, Alastuey A, Angel L, Mar V (2006) Geochemical and statistical analysis of trace metals in atmospheric particulates in Wuhan, central China. Environ Geol 51:121–132. https://doi.org/10.1007/s00254-006-0310-5

WHO (2016) Ambient air pollution: a global assessment of exposure and burden of diseases. Switzerland, Geneva

Wu C, JZ Y (2016) Determination of primary combustion source organic carbon-to-elemental carbon (OC/EC) ratio using ambient OC and EC measurements: secondary OC-EC correlation minimization method. Atmos Chem Phys 16:5453–5465. https://doi.org/10.5194/acp-16-5453-2016

Wu M, Wu D, Fan Q, Wang BM, Li HW, Fan SJ (2013) Observational studies of the meteorological characteristics associated with poor air quality over the Pearl River Delta in China. Atmos Chem Phys 13: 10755–10766. https://doi.org/10.5194/acp-13-10755-2013

Xu WY, Zhao CS, Ran L, Deng ZZ, Liu PF, Ma N, Lin WL, Xu XB, Yan P, He X et al (2011) Characteristics of pollutants and their correlation

to meteorological conditions at a suburban site in the North China Plain. Atmos Chem Phys 11:4353–4369. https://doi.org/10.5194/acp-11-4353-2011

Zeng C, Liu Y, Stein A, Jiao L (2015) Characterization and spatial modeling of urban sprawl in the Wuhan metropolitan area, China. Int J Appl Earth Obs Geoinf 34:10–24. https://doi.org/10.1016/j.jag.2014.06.012

Zhang YL, Cao F (2015) Fine particulate matter (PM2.5) in China at a city level. Nat Sci Reports 5:14884. https://doi.org/10.1038/srep14884

Zhang Y, Zeng L, Wei Y, Liu Y (2008) Characteristics of particulate carbon emissions from real-world Chinese coal combustion.

Environ Sci Technol 42:5068–5073. https://doi.org/10.1021/es7022576

Zhang Z, Wang W, Cheng M, Liu S, Xu J, He Y and Meng F (2017) The contribution of residential coal combustion to PM 2.5 pollution over China's Beijing-Tianjin-Hebei region in winter. Atmos Environ. doi: https://doi.org/10.1016/j.atmosenv.2017.03.054

Zhangxiong Z, Ke H, Zhen H, Ting Y, Longjiao S (2014) Characteristic analysis of OC and EC in PM2.5 of typical haze weather in Wuhan City. Meteorol. Environ Res 5:10–13

Zhou L, Xu X, Ding G, Zhou M, Cheng X (2005) Diurnal variations of air pollution and atmospheric boundary layer structure in Beijing during winter 2000/2001. Adv Atmos Sci 22:126–132